Available online at www.sciencedirect.com

ScienceDirect

Energy Procedia 158 (2019) 2524–2529

Energy Procedia

www.elsevier.com/locate/procedia

10th International Conference on Applied Energy (ICAE2018), 22-25 August 2018, Hong Kong, China

A Combined Central and Local Voltage Control Strategy of Soft Open Points in Active Distribution Networks

Peng Li[a], Haoran Ji[a], Guanyu Song[a,]*, Mingkun Yao[a], Chengshan Wang[a], Jianzhong Wu[b]

[a]*Key Laboratory of Smart Grid of Ministry of Education, Tianjin University, Tianjin 300072, China*
[b]*Institute of Energy, School of Engineering, Cardiff University, Cardiff CF24 3AA, UK*

Abstract

With the increasing penetration of distributed generation (DG), the risk of voltage violations in active distribution networks (ADNs) has become a major concern for the system operator. Soft open point (SOP) is a flexible power electronic device which can realize accurate active and reactive power flow control. This paper proposes a combined central and local operation strategy of SOPs to realize voltage control in ADNs. The active power of SOPs is centrally adjusted based on the information and forecasting throughout the network, which aims to maintain the voltage within the limits in the global optimization. And the local control of reactive power based on real-time measurements can rapidly respond to the frequent voltage violations caused by the fluctuations of DG outputs. The potential benefits of SOPs are fully explored to reduce power losses and improve voltage profile of ADNs. By applying convex relaxation, the original mixed-integer nonlinear programming (MINLP) model is converted into an effectively solved mixed-integer second-order cone programming (MISOCP) model. Case studies on the PG&E 69-node distribution system are conducted to verify the effectiveness of the proposed method.

Keywords: active distribution network (ADN); distributed generation (DG); soft open point (SOP); local voltage control; mixed-integer second-order cone programming

1. Introduction

With the increasing penetration of distributed generation (DG), the risk of voltage violations in active distribution networks (ADNs) has become a major concern for the system operator [1]. In current distribution networks, voltage violations generally are mitigated by dispatching various VAR devices such as the on-load tap changer (OLTC) and

* Corresponding author. Tel.: +86 158 2283 1879; fax: +86 22 27892810.
E-mail address: gysong@tju.edu.cn.

10.1016/j.egypro.2019.01.410

Nomenclature

Sets		$V_i^{\mathrm{q,min}}, V_i^{\mathrm{q,max}}$	set points of the dead-zone in $Q-V$ curve
Ω_{b}	set of all branches	$a_{t,i,n}, d_{t,i,n}$	continuous/binary variables used in the piecewise linearization of $Q-V$ curve
Indices		***Parameters***	
i, j	indices of nodes, from 1 to N_{N}	N_{T}	total periods of the time horizon
t	indices of time periods, from 1 to N_{T}	N_{N}	total number of the nodes
Variables		$P_{t,i}^{\mathrm{LOAD}}, Q_{t,i}^{\mathrm{LOAD}}$	active/reactive power consumption
$P_{t,ji}, Q_{t,ji}$	active/reactive power flow of branch	S_i^{SOP}	capacity limit of SOP
$I_{t,ij}, I_{2,t,ji}$	branch current magnitude and its square	R_{ij}, X_{ij}	resistance/reactance of branch
$U_{t,i}, U_{2,t,i}$	node voltage magnitude and its square	$V^{\max}, V^{\min}$	upper/lower limit of statutory voltage
$P_{t,i}, Q_{t,i}$	total active/reactive power injection	$V_{\mathrm{thr}}^{\max}, V_{\mathrm{thr}}^{\min}$	upper/lower limit of desired voltage range
$P_{t,i}^{\mathrm{SOP}}, Q_{t,i}^{\mathrm{SOP}}$	active/reactive power injection by SOP	A_i^{SOP}	loss coefficient of SOP
$P_{t,i}^{\mathrm{DG}}, Q_{t,i}^{\mathrm{DG}}$	active/reactive power capacity of DG	α, β	weight coefficients
$P_{t,i}^{\mathrm{SOP,L}}$	active power losses of SOP		

switchable capacitor banks (CBs), which usually provide a slow response and a discrete voltage regulation. However, it is difficult to meet the requirement of the fast voltage control by such conventional VAR devices when DGs fluctuate frequently in ADNs [2].However, the rapid development of power electronic technologies provides opportunities for the further optimization of ADNs' operation. Soft open point (SOP) is a novel power electronic device to realize the flexible connection between feeders [3]. SOP can accurately realize the fast power flow control and continuous voltage regulation. Thus, it is of significance to study the strategies of SOPs for voltage control in ADNs.

In general, the central control for SOPs is usually adopted in ADNs. The central control relies on the information and forecasting of the whole system to realize global optimization, which heavily aggravates the computation and communication burdens and consequently might hinder fast response in large networks. Whereas, the local control method, compared with central control, has significant advantages of non-communication, high computation efficiency and strong reliability, which is suitable for the real-time response to the fluctuations.

Thus, a combined central and local voltage control method of SOPs in ADNs is proposed in this paper. The active power of SOPs is centrally adjusted based on the information and forecasting throughout the network, which aims to maintain the voltage within the limits in the global optimization. And the local control of reactive power based on real-time measurements can rapidly respond to the frequent voltage violations caused by the fluctuations of DG outputs. The potential benefits of SOPs are fully explored to reduce power losses and improve voltage profile of ADNs. By applying convex relaxation, the original mixed-integer nonlinear programming (MINLP) model is converted into an effectively solved mixed-integer second-order cone programming (MISOCP) model. Finally, the effectiveness of the combined method is validated on the PG&E 69-node distribution system.

2. Combined central and local operation strategy of SOPs

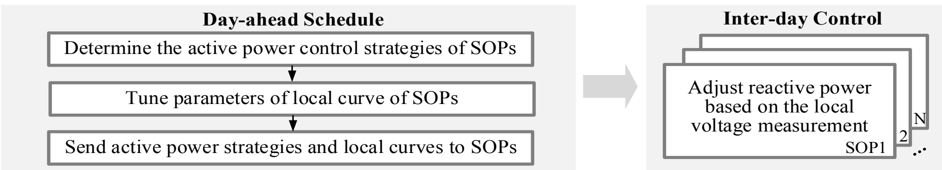

Fig. 1. Schematic of the combined central and local operation strategy of SOPs.

The schematic of the combined strategy of SOPs is shown in Fig.1. Based on the acquired information, the active power control strategies and parameters of local control curves for SOPs can be determined by DMS in the day-ahead schedule. While in the inter-day operation, SOPs adjust the reactive power compensation in real-time, based on the local voltage measurements to maintain both the system losses and the voltages at the desired level.

3. Voltage control problem formulation with SOPs

In this section, a voltage control model with SOPs is built, which realizes the objective economic efficiency and a desired voltage profile of ADNs. The widely used $Q-V$ curve [4] is adopted to realize the local reactive power control of SOPs.

3.1. Mathematic description of combined strategy of SOPs

1) Objective function

A linear weighted combination of minimum total power losses and voltage deviations is taken as the objective function, which is formulated as follows.

$$\min f = \alpha f_{\mathrm{L}} + \beta f_{\mathrm{V}} \tag{1}$$

where the power losses f_{L} and the extent of voltage deviation f_{V} are formulated as:

$$f_{\mathrm{L}} = \sum_{t=1}^{N_{\mathrm{T}}} \sum_{ij\in\Omega_{\mathrm{b}}} R_{ij} I_{t,ij}^2 + \sum_{i=1}^{N_{\mathrm{N}}} P_{t,i}^{\mathrm{SOP,L}} \tag{2}$$

$$f_{\mathrm{V}} = \sum_{t=1}^{N_{\mathrm{T}}} \sum_{i=1}^{N_{\mathrm{N}}} \left|V_{t,i}^2 - 1\right| : (V_{t,i} \geq V_{\mathrm{thr}}^{\max} || V_{t,i} \leq V_{\mathrm{thr}}^{\min}) \tag{3}$$

Equation (3) indicates the threshold function reflecting the extent of voltage deviation. The weight coefficients α and β in equation (1) can be determined by analytic hierarchy process (AHP) and satisfy $\alpha + \beta = 1$

2) System power flow constraints

$$\sum_{ji\in\Omega_{\mathrm{b}}} \left(P_{t,ji} - R_{ji} I_{t,ji}^2\right) + P_{t,i} = \sum_{ik\in\Omega_{\mathrm{b}}} P_{t,ik} \tag{4}$$

$$\sum_{ji\in\Omega_{\mathrm{b}}} \left(Q_{t,ji} - X_{ji} I_{t,ji}^2\right) + Q_{t,i} = \sum_{ik\in\Omega_{\mathrm{b}}} Q_{t,ik} \tag{5}$$

$$V_{t,i}^2 - V_{t,j}^2 + \left(R_{ij}^2 + X_{ij}^2\right) I_{t,ij}^2 = 2\left(R_{ij} P_{t,ij} + X_{ij} Q_{t,ij}\right) \tag{6}$$

$$I_{t,ij}^2 V_{t,i}^2 = P_{t,ij}^2 + Q_{t,ij}^2 \tag{7}$$

$$P_{t,i} = P_{t,i}^{\mathrm{DG}} + P_{t,i}^{\mathrm{SOP}} - P_{t,i}^{\mathrm{LOAD}} \tag{8}$$

$$Q_{t,i} = Q_{t,i}^{\mathrm{DG}} + Q_{t,i}^{\mathrm{SOP}} - Q_{t,i}^{\mathrm{LOAD}} \tag{9}$$

Constraints (4) and (5) represent the active and reactive power balance of node i at period t .The Ohm's law over branch ij at time t is expressed as (6). The current magnitude of each line can be determined by (7). Constraints (8) and (9) indicate the total active and reactive power injection of node i at period t.

3) Secure operation constraints

$$(V^{\min})^2 \leq V_{t,i}^2 \leq (V^{\max})^2, I_{t,ij}^2 \leq (I^{\max})^2 \tag{10}$$

4) SOP operation constraints

The operation constraints of SOPs mainly include the central control of the active power of SOPs and the local Q-V control of reactive power of SOPs.

Central control of the active power of SOPs:

$$P_{t,i}^{\mathrm{SOP}} + P_{t,j}^{\mathrm{SOP}} + P_{t,i}^{\mathrm{SOP,L}} + P_{t,j}^{\mathrm{SOP,L}} = 0 \tag{11}$$

$$P_{t,i}^{\mathrm{SOP,L}} = A_i^{\mathrm{SOP}} \sqrt{\left(P_{t,i}^{\mathrm{SOP}}\right)^2 + \left(Q_{t,i}^{\mathrm{SOP}}\right)^2}, P_{t,j}^{\mathrm{SOP,L}} = A_j^{\mathrm{SOP}} \sqrt{\left(P_{t,j}^{\mathrm{SOP}}\right)^2 + \left(Q_{t,j}^{\mathrm{SOP}}\right)^2} \tag{12}$$

Local $Q-V$ curve control of the reactive power of SOPs:

$$\frac{Q_{t,i}^{\mathrm{SOP}}}{Q_{t,i}^{\mathrm{SOP,max}}} = \varphi\left(V_{t,i}\right), \frac{Q_{t,j}^{\mathrm{SOP}}}{Q_{t,j}^{\mathrm{SOP,max}}} = g\left(V_{t,j}\right) \tag{13}$$

$$\varphi\left(V_{t,i}\right) = \begin{cases} 1.0 & V_{t,i} \in [0, 0.9) \\ \frac{1}{0.9 - V_i^{\mathrm{q,min}}} V_{t,i} + \frac{V_i^{\mathrm{q,min}}}{V_i^{\mathrm{q,min}} - 0.9} & V_{t,i} \in [0.9, V_i^{\mathrm{q,min}}) \\ 0 & V_{t,i} \in [V_i^{\mathrm{q,min}}, V_i^{\mathrm{q,max}}) \\ \frac{1}{V_i^{\mathrm{q,max}} - 1.1} V_{t,i} + \frac{V_i^{\mathrm{q,max}}}{1.1 - V_i^{\mathrm{q,max}}} & V_{t,i} \in [V_i^{\mathrm{q,max}}, 1.1) \\ -1.0 & V_{t,i} \in [1.1, 1.2] \end{cases} \tag{14}$$

The 6-point broken line constitutes $Q-V$ curve, represented by mathematical expression $\varphi\left(V_{t,i}\right)$ and $g\left(V_{t,i}\right)$. For simplicity, $\varphi\left(V_{t,i}\right)$ is taken as an example to be explained, shown as constraint (14). $\left[V_i^{\mathrm{q,min}}, V_i^{\mathrm{q,max}}\right]$ is the dead-zones of the curve where inverters don't supply reactive power. The voltage limits for maximum reactive power provision and absorption are selected as 0.9 p.u. and 1.1 p.u. To determine $Q-V$ curve, only two parameters $V_i^{\mathrm{q,min}}$ and $V_i^{\mathrm{q,max}}$ are required to be set.

The reactive power outputs of SOPs should satisfy their own capacity constraints, described as (15).

$$Q_{t,i}^{\mathrm{SOP,max}}=\sqrt{(S_i^{\mathrm{SOP}})^2-\left(P_{t,i}^{\mathrm{SOP}}\right)^2},\ Q_{t,j}^{\mathrm{SOP,max}}=\sqrt{(S_j^{\mathrm{SOP}})^2-\left(P_{t,j}^{\mathrm{SOP}}\right)^2} \tag{15}$$

As a consequence, constraints (1)-(15) form the optimization model of voltage control with SOPs. It is essentially a large-scale MINLP problem, which requires to be solved accurately and efficiently.

3.2. Conversion to an MISOCP Model

In this section, the original MINLP model is converted into an MISOCP model using the convex relaxation. First, let $U_{2,t,i}$ and $I_{2,t,ij}$ denote the quadratic terms $V_{t,i}^2$ and $I_{t,ij}^2$. Linearized functions are expressed as follows:

$$\sum_{ji\in\Omega_b}\left(P_{t,ji}-R_{ji}I_{2,t,ji}\right)+P_{t,i}=\sum_{ik\in\Omega_b}P_{t,ik} \tag{16}$$

$$\sum_{ji\in\Omega_b}\left(Q_{t,ji}-X_{ji}I_{2,t,ji}\right)+Q_{t,i}=\sum_{ik\in\Omega_b}Q_{t,ik} \tag{17}$$

$$U_{2,t,i}-U_{2,t,j}+\left(R_{ij}^2+X_{ij}^2\right)I_{2,t,ij}=2\left(R_{ij}P_{t,ij}+X_{ij}Q_{t,ij}\right) \tag{18}$$

$$I_{2,t,ji}U_{2,t,i}=P_{t,ij}^2+Q_{t,ij}^2 \tag{19}$$

$$(V^{\min})^2\le U_{2,t,i}\le(V^{\max})^2,\ I_{2,t,ij}\le(I^{\max})^2 \tag{20}$$

$$f_{\mathrm{L}}=\sum_{t=1}^{N_{\mathrm{T}}}\left(\sum_{ij\in\Omega_{\mathrm{b}}}R_{ij}I_{2,t,ij}+\sum_{i=1}^{N_{\mathrm{N}}}P_{t,i}^{\mathrm{SOP,L}}\right) \tag{21}$$

Then (19) can be relaxed to the following second-order cone constraint:

$$\left\|\begin{bmatrix}2P_{t,ij} & 2Q_{t,ij} & I_{2,t,ij}-U_{2,t,i}\end{bmatrix}^{\mathrm{T}}\right\|_2\le I_{2,t,ij}+U_{2,t,i} \tag{22}$$

Auxiliary variable $A_{t,i}$ is introduced to linearized constraint (3). Some relevant constraints are added as follows.

$$f_{\mathrm{V}}=\sum_{t=1}^{N_{\mathrm{T}}}\sum_{i=1}^{N_{\mathrm{N}}}A_{t,i},\ A_{t,i}\ge0 \tag{23}$$

$$A_{t,i}\ge U_{2,t,i}-(V_{\mathrm{thr}}^{\max})^2,\ A_{t,i}\ge-U_{2,t,i}+\left(V_{\mathrm{thr}}^{\min}\right)^2 \tag{24}$$

The expressions of curves $\varphi(V_{t,i})$ and $g(V_{t,j})$ have been exactly modeled based on piecewise linearization [5]. For simplicity, $\varphi(V_{t,i})$ is taken as an example to be explained below. Continuous variables $a_{t,i,n}$ and integer variables $d_{t,i,n}$ are introduced as follows.

$$V_{t,i}=0.8a_{t,i,1}+0.9a_{t,i,2}+a_{t,i,3}V_i^{\mathrm{q,min}}+a_{t,i,4}V_i^{\mathrm{q,max}}+1.1a_{t,i,5}+1.2a_{t,i,6} \tag{25}$$

$$\varphi(V_{t,i})=a_{t,i,1}+a_{t,i,2}-a_{t,i,5}-a_{t,i,6} \tag{26}$$

$$a_{t,i,1}\le d_{t,i,1},a_{t,i,6}\le d_{t,i,5} \tag{27}$$

$$a_{t,i,n}\le d_{t,i,n}+d_{t,i,n-1},n=2,3,4,5 \tag{28}$$

$$a_{t,i,n}\ge0,d_{t,i,n}\in\{0,1\} \tag{29}$$

$$\sum_{n=1}^{6}a_{t,i,n}=1,\sum_{n=1}^{5}d_{t,i,n}=1 \tag{30}$$

As for the nonlinear product terms $a_{t,i,3}^{\mathrm{q}}V_i^{\mathrm{q,min}}$, $a_{t,i,4}^{\mathrm{q}}V_i^{\mathrm{q,max}}$, integer variables $c_{i,1}$ and $c_{i,2}$ are introduced.

$$a_{t,i,3}V_i^{\mathrm{q,min}}=0.90a_{t,i,3}+0.01a_{t,i,3}c_{i,1},0\le c_{i,1}\le20 \tag{31}$$

$$a_{t,i,4}V_i^{\mathrm{q,max}}=0.90a_{t,i,4}+0.01a_{t,i,4}c_{i,2},0\le c_{i,2}\le20 \tag{32}$$

Binary variables $l_{i,1,m}$, $l_{i,2,m}$ are introduced as $a_{t,i,3}c_{i,1}$, $a_{t,i,4}c_{i,2}$ are still the nonlinear product terms.

$$a_{t,i,3}c_{i,1}=\sum_{m=0}^{4}2^m a_{t,i,3}l_{i,1,m} \tag{33}$$

$$a_{t,i,4}c_{i,2}=\sum_{m=0}^{4}2^m a_{t,i,4}l_{i,2,m} \tag{34}$$

Auxiliary variables $w_{t,i,1,m}=a_{t,i,3}l_{i,1,m}$, $w_{t,i,2,m}=a_{t,i,4}l_{i,2,m}$ are further introduced as follows.

$$a_{t,i,3}-\left(1-l_{i,1,m}\right)\mathrm{M}\le w_{t,i,1,m}\le a_{t,i,3} \tag{35}$$

$$a_{t,i,4}-\left(1-l_{i,2,m}\right)\mathrm{M}\le w_{t,i,2,m}\le a_{t,i,4} \tag{36}$$

$$0\le w_{t,i,1,m}\le l_{i,1,m}\mathrm{M},0\le w_{t,i,2,m}\le l_{i,2,m}\mathrm{M} \tag{37}$$

The operation constraints of SOP in (12) can be transformed into the rotated quadratic cone constraints:

$$\left(P_{t,i}^{\mathrm{SOP}}\right)^2+\left(Q_{t,i}^{\mathrm{SOP}}\right)^2\le2\frac{P_{t,i}^{\mathrm{SOP,L}}}{\sqrt{2}A_i^{\mathrm{SOP}}}\frac{P_{t,i}^{\mathrm{SOP,L}}}{\sqrt{2}A_i^{\mathrm{SOP}}} \tag{38}$$

$$\left(P_{t,j}^{\mathrm{SOP}}\right)^2+\left(Q_{t,j}^{\mathrm{SOP}}\right)^2 \le 2\frac{P_{t,j}^{\mathrm{SOP,L}}}{\sqrt{2}A_j^{\mathrm{SOP}}}\frac{P_{t,j}^{\mathrm{SOP,L}}}{\sqrt{2}A_j^{\mathrm{SOP}}} \tag{39}$$

Now, after the conic relaxation, the original MINLP model is converted into an MISOCP model to realize a rapid and accurate calculation.

4. Case study

In this section, the effectiveness of the proposed method is verified on the modified PG&E 69-node system, as shown in Fig. 2(a). Four photovoltaic generators (PVs) are integrated at node 33,35,52 and 54, with a capacity of 1000kVA each. All the PVs are operated at a unit power factor of 0.9. Two groups of SOPs with a capability of 1000kVA are installed. It is assumed that the loss coefficient of each inverter for SOP is 0.02.

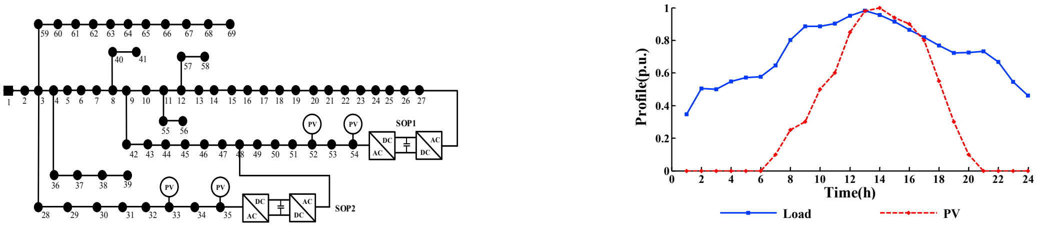

Fig. 2. (a) Structure of the modified PG&E 69-node system. (b) Daily operation curve of PVs and loads

The daily PVs and loads operation curves are shown in Fig.2(b) [6]. The upper and lower limits of statutory voltage range are set as 1.10 p.u. and 0.90 p.u. And the desired voltage range is set from 0.98 p.u. to 1.02 p.u. The weight coefficients α and β are set to 0.7 and 0.3 by AHP.

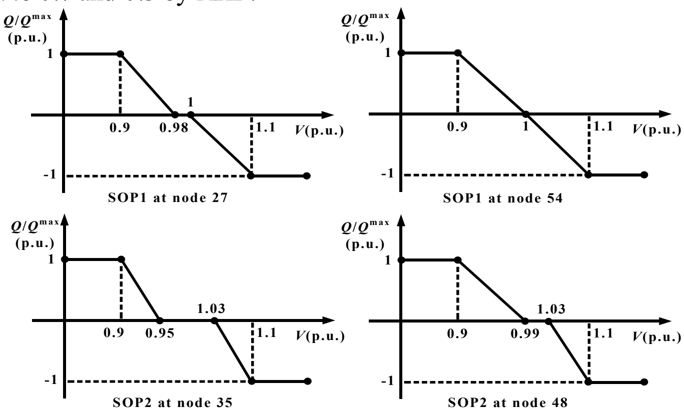

Fig. 3. Local Q-V curve of SOPs

The control parameters of two SOPs are optimally tuned by the proposed method. The optimization results of local $Q-V$ control curves for each SOP are shown in Fig. 3.

Three scenarios are adopted to verify the effectiveness of the proposed strategy in ADNs:

Scenario I: There is no control strategy conducted on SOPs, and the initial operation state of ADNs is obtained.

Scenario II: The proposed combined central and local control strategy is conducted on SOPs.

Scenario III: The outputs of SOPs are regulated by central control strategy to realize global optimization.

Table 1. Optimization results of three scenarios.

	Scenario I	Scenario II	Scenario III
Power losses(kWh)	1758.7	1311.6	1250.5
Minimum voltage of ADN (p.u.)	0.9351	0.9694	0.9701
Maximum voltage of ADN(p.u.)	1.0460	1.0254	1.0252

The outputs of SOPs in Scenario II are shown in Fig. 4 and Fig. 5. The optimization results of three scenarios are listed in Table 1. Compared with Scenario I, the proposed control strategy in Scenario II effectively mitigate voltage deviation and reduce power losses of the whole network. It can be seen that the proposed strategy has a similar performance with the central control strategy in Scenario III, which has the most optimal use of active and reactive outputs of SOPs. Considering the proposed combined control strategy is based on less measurement information, it could reduce the computational burden as well as achieve the near globally optimal solution.

Fig. 4. (a) Active outputs of SOP1. (b) Reactive outputs of SOP1.

Fig. 5. (a) Active outputs of SOP2. (b) Reactive outputs of SOP2.

Fig. 6 shows the voltage profiles of the nodes PVs connected to in three scenarios. Compared with Scenario I, voltage profiles are significantly improved in Scenario II.

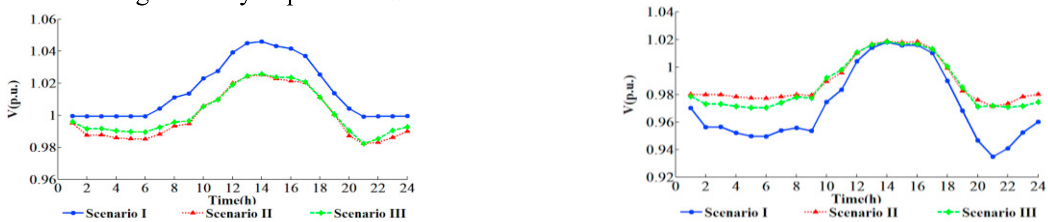

Fig. 6. (a) Voltage profile at node 35. (b) Voltage profile at node 52.

5. Conclusion

This paper proposes a combined central and local operation strategy of SOPs to realize voltage control in ADNs. By applying convex relaxation, the original MINLP model is converted into an effectively solved MISOCP model. The optimization results show that by adopting the proposed combined control strategy, the potential benefits of SOPs are fully explored to reduce power losses and improves voltage profile of ADNs.

Acknowledgements

This work was conducted in cooperation of APPLIED ENERGY UNiLAB-DEM: Distributed Energy & Microgrid. UNiLAB is an international virtual lab of collective intelligence in Applied Energy.

References

[1] Wang X, Wang C, Xu T, et al. Optimal voltage regulation for distribution networks with multi-microgrids. Applied Energy 2018; 210: 1027-36.

[2] Ferreira P D, Carvalho P, Ferreira L A. Distributed energy resources integration challenges in low-voltage networks: voltage control limitations and risk of cascading. IEEE Transactions on Power Systems 2013; 4(1): 82-88.

[3] Wang C, Song G, Li P, et al. Optimal siting and sizing of soft open points in active electrical distribution networks. Applied Energy 2017; 189: 301-309.

[4] Karagiannopoulos S, Aristidou P, Hug G. Hybrid approach for planning and operating active distribution grids. IET Generation Transmission & Distribution 2016; 11(3): 685-95.

[5] Zhao J, Li Y, Li P, et al. Local voltage control strategy of active distribution network with PV reactive power optimization. Proceedings of IEEE PES General Meeting, 2017; 1-5.

[6] Long C, Wu J, Thomas L. Optimal operation of soft open points in medium voltage electrical distribution networks with distributed generation. Applied Energy 2016; 184: 427-437.